

***High Pressure Diffraction Studies
of Gallosilicate Natrolite:
Applications to Pressure-Induced
Cation Trapping.***

By

**Gemma Louise Hill
(née Little)**

A thesis submitted to
The University of Birmingham
for the degree of
Doctor of Philosophy

School of Chemistry
University of Birmingham
2010

UNIVERSITY OF
BIRMINGHAM

University of Birmingham Research Archive

e-theses repository

This unpublished thesis/dissertation is copyright of the author and/or third parties. The intellectual property rights of the author or third parties in respect of this work are as defined by The Copyright Designs and Patents Act 1988 or as modified by any successor legislation.

Any use made of information contained in this thesis/dissertation must be in accordance with that legislation and must be properly acknowledged. Further distribution or reproduction in any format is prohibited without the permission of the copyright holder.

1st of 3 files

Front pages and chapter 1

**The remaining chapters
are in two additional files**

Acknowledgements

A very sincere thank you must go to my supervisor Dr Joseph A. Hriljac,^a for his words of encouragement, academic support, patient teaching methods and always making himself available to help when needed. Many, many thanks.

Thank you to the EPSRC for research funding and the University of Birmingham for the postgraduate research opportunity. Additional project sponsorship came from (BNFL) Nexia solutions, with project support from Dr Ewan Maddrel^b and Dr Neil Hyatt.^c

For Beamline support during Synchrotron X-Ray and Neutron diffraction data collection, I would like to thank Dr William Marshall,^d Dr Alistair Lennie,^e Dr Richard Ibberson^d and Dr YongJae Lee.^f

Thanks to Prof. Mark Smith^g for collection of silicon and gallium NMR data.

For the kind use of the Quickpress equipment I would like to thank Prof. Paul McMillan.^h For data collection and equipment support, thanks go to Dr Edward Bailey of the McMillan Research group.

Thank you for the friendship and support from all the members of Level 5, Department of Chemistry, University of Birmingham. In particular, I'd like to thank Dr Jenny Readman and Maria Thompson.

Personal thanks to my wonderful Parents-in-law for all the hours of baby-sitting that they volunteered so that I could finish writing this thesis. To my patient husband Dr Adrian Hill, thank you in so many ways for all your constant love and support.

^a School of Chemistry, University of Birmingham, Edgbaston, Birmingham

^b Nexia Solutions, Sellafield, Seascale, Cumbria, CA20 1PG.

^c ISL, Department of Engineering Materials, University of Sheffield, Sheffield

^d ISIS, Science and Technology Facilities Council, Rutherford Appleton Laboratory, Didcot, OX11 0QX, UK.

^e Daresbury Laboratory, Daresbury Science & Innovation Campus, Warrington, Cheshire, WA4 4AD, UK.

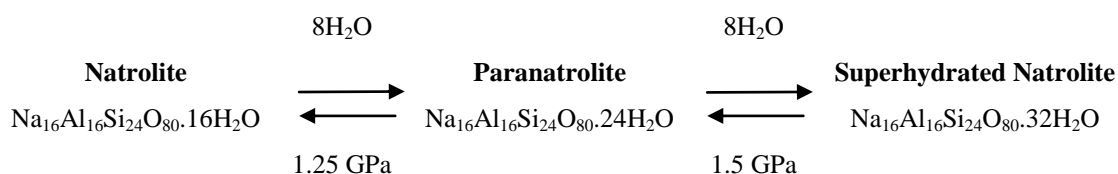
^f National Synchrotron Light Source, Brookhaven National Laboratory, Upton, New York 11973-5000.

^g Department of Physics, University of Warwick, Coventry, CV4 7AL.

^h University College London, Department of Chemistry, 20 Gordon Street, London WC1H 0AJ.

Abstract

The natrolite family of zeolites undergoes volume expansion under pressure. Natrolite itself is a three dimensionally porous zeolite with 8-ring channels. It shows an unusual unit cell volume expansion when under hydrostatic pressure where it undergoes two distinct, reversible phase transitions to parnatrolite and then super-hydrated natrolite.



The behaviour of gallosilicate natrolite, a synthetic analogue of the aluminosilicate mineral, was investigated in this thesis. Two forms exist, orthorhombic (as per the mineral) and tetragonal. These two forms have been synthesised and structurally characterised by powder neutron diffraction and synchrotron X-ray diffraction techniques at ambient pressure to elucidate details of the ordering. In addition, high pressure neutron and synchrotron X-ray diffraction data have been collected on both the tetragonal and the orthorhombic forms. These data confirm pressure-induced hydration and pore swelling in both the gallosilicate materials, as seen in the aluminosilicate form but at much lower pressures. The neutron data has also allowed a full study of the changes in hydrogen-bonding in the normal and superhydrated states.

The natrolite family will not normally undergo ambient ion-exchange due to the small pores and the strongly bound framework cations. Exploitation of the pressure-induced state offered a high pressure ion-exchange route, with trapping of large exchanged cations upon pressure release. Ion exchange investigations using the aluminosilicate and gallosilicate natrolites have provided the first evidence of high pressure cation trapping. Exposure to a saturated CsCl solution at a pressure of 1 GPa and a temperature of 100°C led to cesium trapping within the framework upon pressure release. Back-exchange treatment in a sodium chloride reflux did not leach the trapped caesium. For the aluminosilicate natrolite up to 33% Na/Cs exchange was trapped within the framework via this high pressure exchange method.

Abbreviations

Ga-NAT, Na-GaSi-NAT	Gallosilicate Natrolite
Ga-NAT _{tet}	Tetragonal Gallosilicate Natrolite (Na ₈ Ga ₈ Si ₁₂ O ₄₀ .8H ₂ O)
Ga-NAT _{orth}	Orthorhombic Gallosilicate Natrolite (Na ₁₆ Ga ₁₆ Si ₂₄ O ₈₀ .16H ₂ O)
Al-NAT, Na-AlSi-NAT	Aluminosilicate Natrolite (Na ₁₆ Al ₁₆ Si ₂₄ O ₈₀ .16H ₂ O)
GPa	Giga Pascal
Kbar	Kilo Bars
DAC	Diamond Anvil Cell
PIH	Pressure Induced Hydration
PIE	Pressure Induced Expansion
PXRD	Powder X-Ray Diffraction
FTIR	Fourier Transform Infra-Red
TGA	Thermogravimetric analysis
NMR	Nuclear Magnetic Resonance
SEM	Scanning Electron Microscope
EDX	Electron Dispersive X-Ray
HRPD	High Resolution Powder Diffraction
NSLS	National Synchrotron Light Source
X7a	X7a beamline at the NSLS
9.5HPT	9.5 station High Pressure and Temperature beamline, Daresbury Laboratory.
Pearl	Pearl beamline, ISIS facility, Oxfordshire.

Table of Contents

CHAPTER ONE	1
Introduction	
1.1 Zeolites	2
1.1.1 Zeolite Structure	4
1.2 The Natrolite Family	7
1.2.1 Gallosilicate Zeotypes	10
1.3 The Natrolite Family at High Pressure	13
1.3.1 Aluminosilicate Natrolite	13
1.3.2 Tetranatrolite	15
1.3.3 Mesolite	16
1.3.4 Scolecite	17
1.3.5 Gallosilicate Natrolite	17
1.4 Potential Uses of High-Pressure Superhydration: Aims of This Research	19
1.4.1 Research Included in This Thesis:	20
 CHAPTER TWO	 25
Experimental	
2.1 Diffraction Theory	27
2.1.1 Bragg's Law	28
2.1.2 Diffraction of X-rays and Neutrons	29
2.1.2.1 X-ray Use in Diffraction	29
2.1.2.2 Neutron Use in Diffraction	31
Hydrogen Scattering	33
2.2 Synthesis, Preparation and Characterisation of Materials	34
2.2.1 Hydrothermal Synthesis	34
2.2.1.1 Orthorhombic Na-Ga-Si-NAT	35
2.2.1.2 Tetragonal Na-Ga-Si-NAT	36
2.2.2 Deuteration	37

2.2.2.1 Vacuum Deuteration	37
2.2.2.2 Hydrothermal Deuteration	37
2.2.3 FTIR Spectroscopy	38
2.2.4 NMR	40
2.2.5 TGA	40
2.3 Diffraction Instrumentation and Equipment	41
2.3.1 Bruker D5000	41
2.3.2 High Pressure Diffraction	42
2.3.2.1 Synchrotron X-ray Diffraction	42
Diamond Anvil Cell (DAC)	42
X7a	44
9.5HPT	44
2.3.2.2 Neutron Diffraction	45
Pearl	45
Paris-Edinburgh Cell	46
2.3.3 Ambient Pressure High Resolution Neutron Diffraction, HRPD.	49
2.4 Data Analysis	51
2.4.1 Rietveld	52
2.4.2 EoS	57
2.4.2.1 The Murnaghan Equation of State	58
Units	59
2.4.3 SEM	59
2.4.3.1 Electron Dispersive X-ray Analysis (EDX).	60
2.5 Ion Exchange	63
2.5.1 Ion Exchange at Ambient Pressure	63
2.5.2 Hydrothermal Ion Exchange	63
2.5.3 High Pressure Ion Exchange	64
2.5.3.1 Ion Exchange Using a DAC	64
2.5.3.2 Quick Press Ion Exchange	65
2.5.4 Back-Exchange Reflux	68

CHAPTER THREE

72

Synthesis, Characterisation and Preparation of Na-Ga-Si-NAT

3.1 Synthesis and Optimisation	73
3.1.1 Orthorhombic Ga-Si-NAT	73
3.1.2 Tetragonal Ga-Si-NAT	74
3.2 Indexing and Unit Cell Refinement	76
3.2.1 Orthorhombic Na-Ga-NAT	81
3.2.2 Tetragonal Na-Ga-NAT	82
3.3 TGA	83
3.4 SEM EDX	88
3.5 MAS NMR	92
3.6 Preparation for Neutron Diffraction Studies-Sample Deuteration	98
3.7 High Resolution Neutron Powder Diffraction	102
3.7.1 Orthorhombic Ga-NAT	102
3.7.2 Tetragonal Ga-NAT	106
3.8 Conclusions	108

CHAPTER FOUR

111

High Pressure Powder Neutron Diffraction of Gallosilicate Natrolite

4.1 High Pressure Neutron Diffraction Results	112
4.1.1 Orthorhombic Gallosilicate Natrolite	113
4.1.1.1 Ambient Pressure Refinement	114
Modelling the Water Content and Bonding at Ambient Pressure	115
4.1.1.2 High Pressure Refinement	118
4.1.1.3 Volume Expansion and Superhydration in Orthorhombic Ga-NAT	124
4.1.2 Tetragonal Gallosilicate Natrolite	127
4.1.2.1 Ambient Pressure Refinement	128
Modelling the Water Content and Bonding at Ambient Pressure	129
4.1.2.2 High Pressure Refinement	133

Modelling the Water Content and Bonding at High Pressure	133
4.1.2.3 Volume Expansion and Superhydration in Tetragonal Ga-NAT.	138
4.2 High Pressure Effects upon the Gallosilicate Natrolite Framework	140
4.2.1 Pore Dimensions and Chain Rotation	140
4.2.2 T-O-T Angles	145
4.2.3 Bonding Changes in Orthorhombic Ga-NAT during High Pressure Studies	149
4.2.4 Bonding Changes in Tetragonal Ga-NAT During High Pressure Studies	158
4.3 Bond Valence	166
4.4 Equation of State	170
4.5 Conclusion	173

CHAPTER FIVE

175

High Pressure Synchrotron X-Ray Diffraction

5.1 Synchrotron X-Ray Diffraction Studies (X7A)	177
5.1.1 Capillary Data Results	177
5.1.2 High Pressure Data	180
5.1.2.1 Tetragonal Na-GaSi-NAT	180
5.1.2.2 Orthorhombic Na-GaSi-NAT	182
5.2 Fitting an Equation of State	187
5.3 Synchrotron X-Ray Diffraction Studies (9.5HPT)	189
5.3.1 Ambient Pressure Studies	192
5.3.2 High Pressure Studies	194
5.3.3.1 Orthorhombic Na-GaSi-NAT	194
Compression 0-0.906 GPa	205
Superhydration 0.906 GPa	210
Compression of the Superhydrated Phase 0.906-2.365 GPa	211
Bonding Changes during High Pressure Studies of Orthorhombic Na-GaSi-NAT.	212
Fitting Equations of State to High Pressure Data	215
5.3.3.2 Tetragonal Na-GaSi-NAT	218
Expansion 0-0.727 GPa	226
Compression of the Superhydrated Phase from 0.727-5.108 GPa	231
Bonding Changes during High Pressure Studies of Tetragonal Na-GaSi-NAT.	232

Fitting Equations of State to High Pressure Data	235
5.3.3.3 Quality of Data	238
5.4 Conclusions	239

CHAPTER SIX **241**

Hydrothermal Ion Exchange in Natrolite and Gallosilicate Natrolite

6.1 Introduction	242
6.2 Na/Cs hydrothermal Ion Exchange	245
6.3 Na/Sr Hydrothermal Ion Exchange	252
6.4 Na/Rb Hydrothermal Ion Exchange	259
6.5 Na/Ba Hydrothermal Ion Exchange	266
6.6 Summary	272

CHAPTER SEVEN **274**

High Pressure Ion Exchange

7.1 In-Situ X-ray Diffraction High Pressure Exchange (DAC)	276
7.2 Quickpress Ion Exchange Experiments	279
7.2.1 Quickpress Vs. Diamond Anvil	279
7.2.2 Results and Discussion	280
7.2.2.1 Temperature Dependence	283
Discussion of Temperature Dependence Results	291
7.2.2.2 Time Dependence	294
Discussion of Time Dependence Results	307
7.3 Summary	310

CHAPTER EIGHT **312**

Summary

8.1 High Pressure Data Evaluation and Comparison	316
--	-----

8.1.1 Framework Flexibility-The Mechanism by Which PIH Occurs	321
8.1.2 Reversibility	322
8.2 Ion Exchange Experiments	323
8.3 Summary of New and Original Work Reported In This Thesis.	324
8.4 Conclusions	326
8.5 Further Work	328
8.5.1 High Pressure Behaviour in the Natrolite Family	328
8.5.2 Ion Exchange	328

Appendix

1.1 Rietveld Refinement Profile Plots for High Pressure Neutron Diffraction Data	2
1.2 Rietveld Refinement Profile Plots for High Pressure Synchrotron X-Ray Diffraction data	8
1.2.1 Synchrotron X-Ray Diffraction Data from X7a	8
1.2.2 Synchrotron X-Ray Diffraction Data from 9.5 HPT	14
1.2.2.1 Orthorhombic Ga-NAT	14
1.2.2.2 Tetragonal Ga-NAT	23
1.3 Atoms Drawings from Refined, High Pressure, Synchrotron X-Ray Diffraction Data	33
1.3.1 Orthorhombic Ga-NAT	33
1.3.2 Tetragonal Ga-NAT	39

CHAPTER ONE

Introduction

1.1 Zeolites.....	2
1.1.1 Zeolite Structure.....	4
1.2 The Natrolite Family.....	7
1.2.1 Gallosilicate Zeotypes.....	10
1.3 The Natrolite Family at High Pressure	13
1.3.1 Aluminosilicate Natrolite.....	13
1.3.2 Tetranatrolite.....	15
1.3.3 Mesolite.....	16
1.3.4 Scolecite	17
1.3.5 Gallosilicate Natrolite	17
1.4 Potential Uses of High-Pressure Superhydration: Aims of This Research.....	19
1.4.1 Research Included in This Thesis:	20

1.1 Zeolites

This thesis is based upon the study of the high-pressure properties of a zeolite material called natrolite. The following sections will cover general aspects of zeolites including structures, an introduction to the natrolite family and some previously reported high-pressure studies.

A zeolite is one of a group of microporous materials, having at least one-dimensional porosity in the range of 2-12 Å. By definition, a zeolite is an aluminosilicate which will reversibly take up water molecules. The zeolite family is incredibly diverse in its topology, occurring both naturally and synthetically. Laboratory synthesis of zeolites is often via the hydrothermal method.

The hydrothermal method is a mild temperature and pressure route which mimics the conditions found in the Earth's crust. The hydrothermal method relies upon a sealed system in order to take a mild temperature route. Such a system allows a build in autogeneous pressure within the vessel, by heating of aqueous medium at or above its boiling point.¹ Autogeneous pressures reduce the need for extreme temperatures and therefore offer a route to thermally unstable species not accessible by other solid-state methods. Generally, synthesis involves the formation of a silica based gel which subsequently crystallises under hydrothermal conditions. The identity of the product is not solely dependent upon the stoichiometry of starting materials. In fact, the stoichiometry of the zeolite moieties in the final product is often very different to that of the starting materials. The variables in the hydrothermal environment (e.g. temperature, pH and solvent identity), often show much greater dominance than composition in the reaction outcome.

Zeolites have an overall negatively charged framework of Al, Si and O in the form of corner shared $\text{AlO}_{4/2}^-$ and $\text{SiO}_{4/2}$ tetrahedra. Within the framework there are charge balancing cations and loosely bound water molecules. Zeolites are derived from formula

SiO_2 , where Al^{3+} , a similar sized cation, is substituted into the structure to give an aluminosilicate (Figure 1). In this substitution an overall negative charge is achieved requiring the presence of charge balancing cations which occupy a vacant intrapore site. These aluminosilicates can be described by a general formula given in Equation 1.

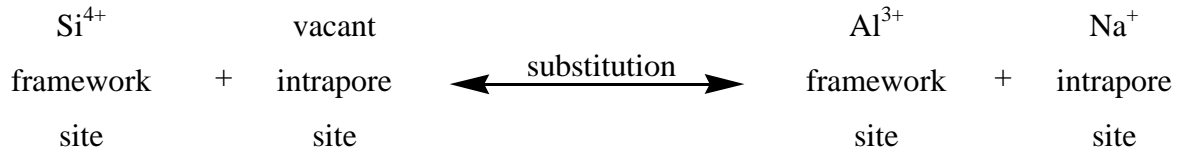
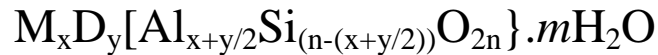


Figure 1: Substitution of aluminium into a silicate.



M = monovalent cation, **D** = divalent cation, **n**=an integer representing the unit cell, typically between 10-100 and **m** = loosely bound water which is reversibly taken up by the zeolite framework.

Equation 1: Structural formula describing zeolite materials.

Strictly, a zeolite is described as an aluminosilicate, but using these principals of substitution a wide variety of related structures (zeotypes) can be synthesised. Synthetic zeotypes of aluminosilicate natrolite (gallosilicate natrolites) are of particular interest in this thesis. It is the orthorhombic and the tetragonal forms of sodium gallosilicate natrolite ($\text{Na}_{16}\text{Ga}_{16}\text{Si}_{24}\text{O}_{80}\cdot 16\text{H}_2\text{O}$ and $\text{Na}_8\text{Ga}_8\text{Si}_{12}\text{O}_{40}\cdot 8\text{H}_2\text{O}$) that will be studied during high-pressure crystallographic investigation. In a later section within this chapter the gallosilicate zeotypes are described in greater detail.

1.1.1 Zeolite Structure

In a zeolite, the Si/Al tetrahedra are made up of a central Si or Al atom (T atom) surrounded by four oxygen atoms. All four of the oxygen atoms within the tetrahedra are shared, each by only two tetrahedra to give an extended structure of Al and Si tetrahedra. Tetrahedra are corner connected through a flexible oxygen bridge. The flexibility of the bridging T-O-T bond (T=Al or Si), means that the tetrahedra can combine in a number of different ways to give huge structural variety in the zeolite family. Arrangement of these tetrahedra to form zeolite structures can be described in terms of primary and secondary building units. The primary building unit is the TO_4 tetrahedra and these units are arranged to give a variety of secondary building units, in turn these units can combine to give the larger zeolite structure^{2,3,4,5} (Figure 2 to Figure 4).

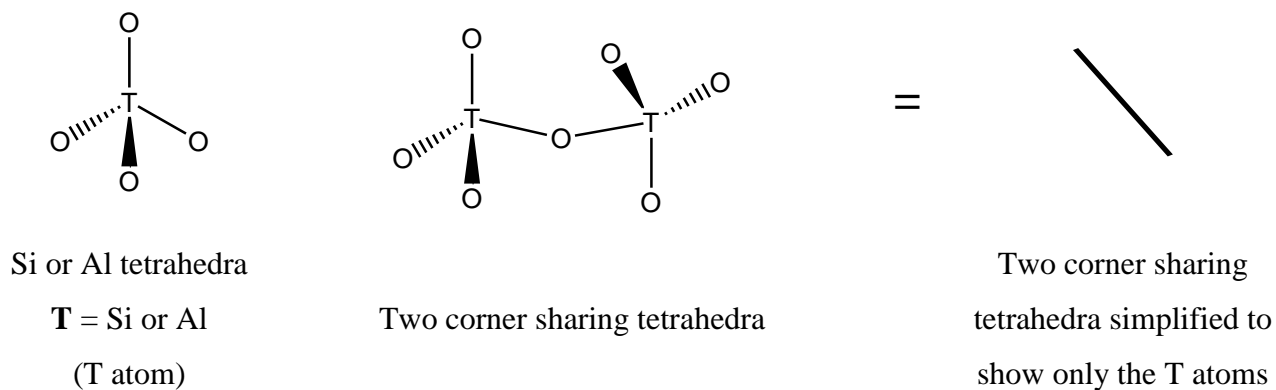


Figure 2: Connection of primary building units to give a secondary structure.

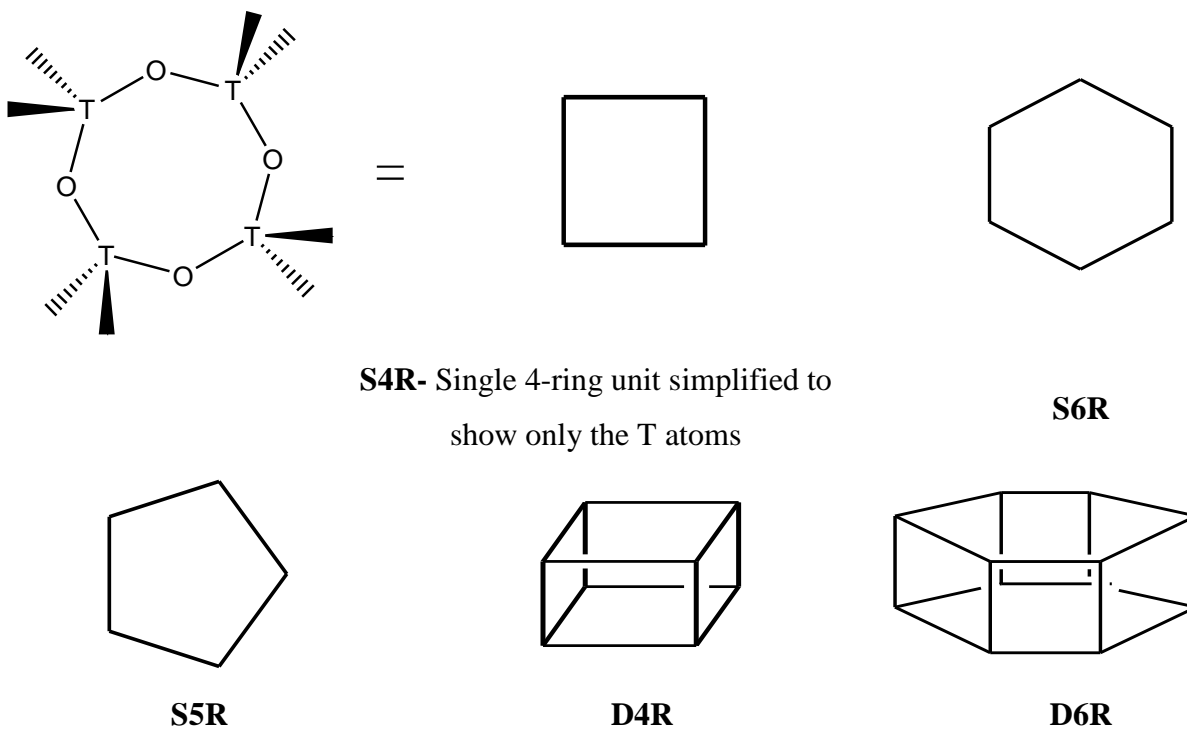
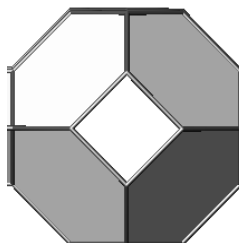


Figure 3: Secondary building units.

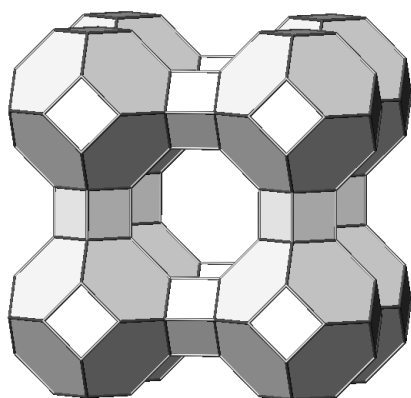
S=single, D=double, R=ring.

Secondary building units can combine to give larger structures



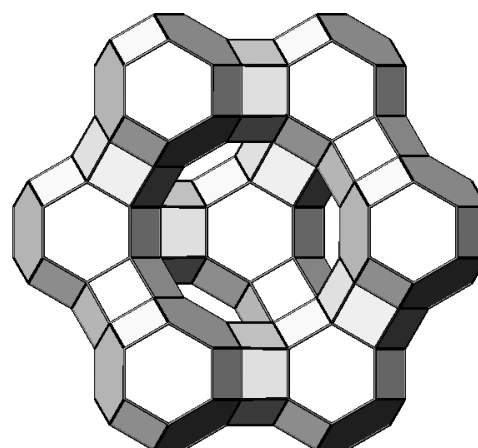
α -sodalite cage

S4R and S6R secondary units combine to give this cage-like structure.



Zeolite LTA

Unit cell structure comprising sodalite cages
linked by D4R, with an 8-ring aperture.



Faujasite

Unit cell structure comprising sodalite cages
linked by D6R, with a 12-ring aperture.

Figure 4: Larger structures: cages and zeolites.

1.2 The Natrolite Family

Natrolite ($\text{Na}_{16}\text{Al}_{16}\text{Si}_{24}\text{O}_{80} \cdot 16\text{H}_2\text{O}$) occurs widely in nature and is often found in association with analcime.⁶ The framework of natrolite is similar to that of gonnardite, mesolite and scolecite², which are all considered members of the same zeolitic family-the natrolite family. The natrolite framework (Figure 5) is comprised of linked fibrous chains; these chains consist of T_5O_{10} units connected along the c -axis. The fibrous chains are linked to produce helical 8-ring pores which extend along the c -axis.⁷ Within the natrolite unit cell there are 16 cations and water molecules present within the zeolitic pores. Within the pores each sodium cation is bonded to four framework oxygens and two water molecules. The weak nature of the fibrous chain connections gives rise to some diverse structural variations.^{4,6,8,10,11,12}

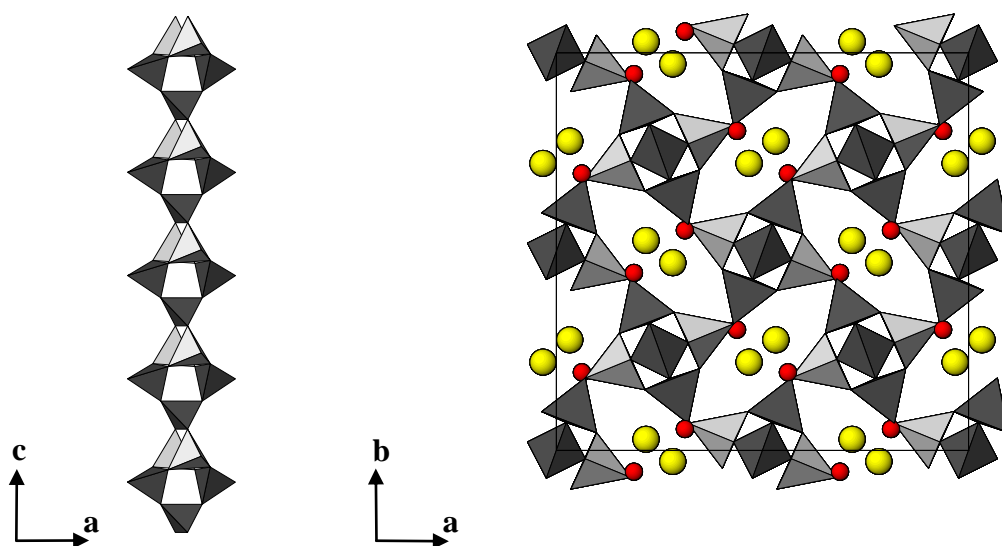


Figure 5: a) schematic of a 'fibrous' natrolite chain. b) Schematic of the unit cell of aluminosilicate natrolite. Atomic coordinates for natrolite were used from a report by Artioli.⁸ In each case, polyhedra represent Si (dark grey) and Al (light grey) oxide tetrahedra. Water molecules represented by an oxygen atom (red). Yellow atoms represent charge balancing cations Na^+ .

The mineral members of the natrolite family, sharing the same structural topology, are very similar in composition. A comparative structural summary of the natrolite family can be seen in Table 1. Generally symmetry, cell size and pore apertures are all very similar. The most significant difference between the natrolite family members occurs in the nature and stoichiometry of the framework charge balancing cations and the intrapore water content e.g. two sodium cations (2Na^+) are readily replaced by one calcium cation (1Ca^{2+}), more space is freed within the pores so there is an increase in intrapore water content. When comparing natrolite ($\text{Na}_{16}\text{Al}_{16}\text{Si}_{24}\text{O}_{80}\cdot 16\text{H}_2\text{O}$) with an analogous calcium substituted form: scolecite ($\text{Ca}_8\text{Al}_{16}\text{Si}_{24}\text{O}_{80}\cdot 24\text{H}_2\text{O}$); we can see a reduction in symmetry from orthorhombic to monoclinic. In natrolite there is an infinite Na-OW-Na bridging water oxygen bond which extends throughout the structure along the *c*-axis. In scolecite these infinite bonds are replaced by isolated $\text{Ca}^{2+}(\text{H}_2\text{O})_3$ complexes. Gonnardite and mesolite contain both infinite and localised bonding modes, relative to the Na/Ca ratio⁹. The difference in the nature of these intrapore cations can result in deformations/alterations to the ideal natrolite framework structure. In the case of scolecite (fully calcium substituted natrolite), the framework is distorted to give a more elliptical pore shape when compare to the ideal $\text{Na}_{16}\text{Al}_{16}\text{Si}_{24}\text{O}_{80}\cdot 16\text{H}_2\text{O}$ structure.

The degree of hydration also effects the structure, for example paranatrolite ($\text{Na}_{16-x}\text{Ca}_x(\text{Al}_{16+x}\text{Si}_{24-x}\text{O}_{80})\cdot n\text{H}_2\text{O}$, ideally $x=0$, $n=24$), can be considered as a hydrated form of natrolite ($\text{Na}_{16}(\text{Al}_{16}\text{Si}_{24}\text{O}_{80})\cdot 16\text{H}_2\text{O}$), but has a very different unit cell. Paranatrolite can dehydrate to metastable tetranatrolite ($\text{Na}_{16-x}\text{Ca}_x(\text{Al}_{16+x}\text{Si}_{24-x}\text{O}_{80})\cdot n\text{H}_2\text{O}$, $x=2.4-3.9$, $n=16$); yet another structural change as a result of altered hydration.¹⁰

Table 1: Structural and crystallographic data on Natrolite family.^{2,4}

Natrolite	$\text{Na}_{16}(\text{Al}_{16}\text{Si}_{24}\text{O}_{80}) \cdot 16\text{H}_2\text{O}$
Structure	Two dimensional 8-membered rings parallel to <i>c</i> -axis
Crystal Symmetry	Orthorhombic
Space group	<i>Fdd2</i>
Lattice parameters ⁸ (Å)	$a=18.272, b=18.613, c=6.593$

Tetranatrolite¹⁰	$\text{Na}_{16-x}\text{Ca}_x(\text{Al}_{16+x}\text{Si}_{24-x}\text{O}_{80}) \cdot n\text{H}_2\text{O}, x=2.4-3.9, n=16$
Structure	Two dimensional 8-membered rings parallel to <i>c</i> -axis
Crystal Symmetry	tetragonal
Space group	<i>I42d</i> or <i>I4₁md</i>
Lattice parameters ¹⁰ (Å)	$a=13.197, c=6.630$

Mesolite	$\text{Na}_{16}\text{Ca}_{16}\text{Al}_{48}\text{Si}_{72}\text{O}_{240} \cdot 64\text{H}_2\text{O}$
Structure	Two dimensional 8-membered rings parallel to <i>c</i> -axis
Crystal Symmetry	orthorhombic
Space group	<i>Fdd2</i>
Lattice parameters ⁴ (Å)	$a=56.7, b=6.54, c=18.44$

Paranatrolite¹¹	$\text{Na}_{16-x}\text{Ca}_x(\text{Al}_{16+x}\text{Si}_{24-x}\text{O}_{80}) \cdot n\text{H}_2\text{O}, \text{ ideally } x=0, n=24$
Structure	Two dimensional 8-membered rings parallel to <i>c</i> -axis
Crystal Symmetry ^{12,13}	Monoclinic or Pseudo-orthorhombic
Space group	<i>Cc</i> or <i>Fd</i>
Lattice parameters ⁴ (Å)	$a=13.19, b=13.32, c=6.55$

Gonnardite	$\text{Na}_4\text{Ca}_2(\text{Al}_8\text{Si}_{12}\text{O}_{80}) \cdot 14\text{H}_2\text{O}$
Structure	Two dimensional 8-membered rings parallel to <i>c</i> -axis
Crystal Symmetry	Orthorhombic
Space group	<i>I42d</i>
Lattice parameters ⁴ (Å)	$a=13.19, b=13.32, c=6.55$

Scolecite	$(\text{Ca}_8\text{Al}_{16}\text{Si}_{24}\text{O}_{80} \cdot 24\text{H}_2\text{O})$
Structure	Two dimensional 8-membered rings parallel to <i>c</i> -axis
Crystal Symmetry	monoclinic
Space group	<i>Cc</i>
Lattice parameters ⁴ (Å)	$a=18.53, b=18.99, c=6.56, \beta=90.39^\circ$

1.2.1 Gallosilicate Zeotypes

Gallium silicates can easily be formed by substitution of aluminium for gallium in a pre-crystalline zeolite gel.⁴ Gallium is directly below aluminium in the periodic table (both 3^+ cations). They form isoelectric $\text{GaO}_{4/2}^-$ and $\text{AlO}_{4/2}^-$ tetrahedra, and are therefore chemically similar. When substituting species into a zeolite reaction mixture to form products isostructural to an aluminosilicate, the substituted species should be chemically similar to aluminium for successful synthesis. Substituting very different species into the reaction can result in much reduced crystallisation.² This correlates with the dependence of crystallisation of zeolites upon the Si/Al ratio. Chemically similar species can maintain this ratio by “mimicking” aluminium. The recent interest in powerful structure-directing groups means more and more diverse non-aluminosilicates have been synthesised.

In this thesis, gallosilicate analogues of natrolite ($\text{Na}_{16}\text{Al}_{16}\text{Si}_{24}\text{O}_{80} \cdot 16\text{H}_2\text{O}$) are used in high-pressure crystallographic investigations. There are two synthetic forms of gallosilicate natrolite, orthorhombic ($\text{Na}_{16}(\text{Ga}_{16}\text{Si}_{24}\text{O}_{80}) \cdot 16\text{H}_2\text{O}$) and tetragonal ($\text{Na}_8\text{Ga}_8\text{Si}_{12}\text{O}_{40} \cdot 8\text{H}_2\text{O}$).^{14,15} These forms differ only in the ordering of the T atoms (Si or Ga). The orthorhombic form has ordered T sites so that Si and Ga have separate atomic sites. The tetragonal form has disorder over these T-sites so that each site is shared by Si and Ga in a 3:2 ratio. The structure of each gallosilicate natrolite is given in Figure 6 and Figure 7. These structures come from the diffraction studies discussed in chapters 3, 4 and 5. The synthesis of these zeotypes is included in chapter 2; details are given in accordance with the method outlined by the IZA synthesis commission.¹⁶ These zeotypes will be investigated at high-pressure in the hope that they will show similar high pressure behaviour to that of the aluminosilicate zeolite parent. This previously reported, high-pressure behaviour is discussed in the next section.

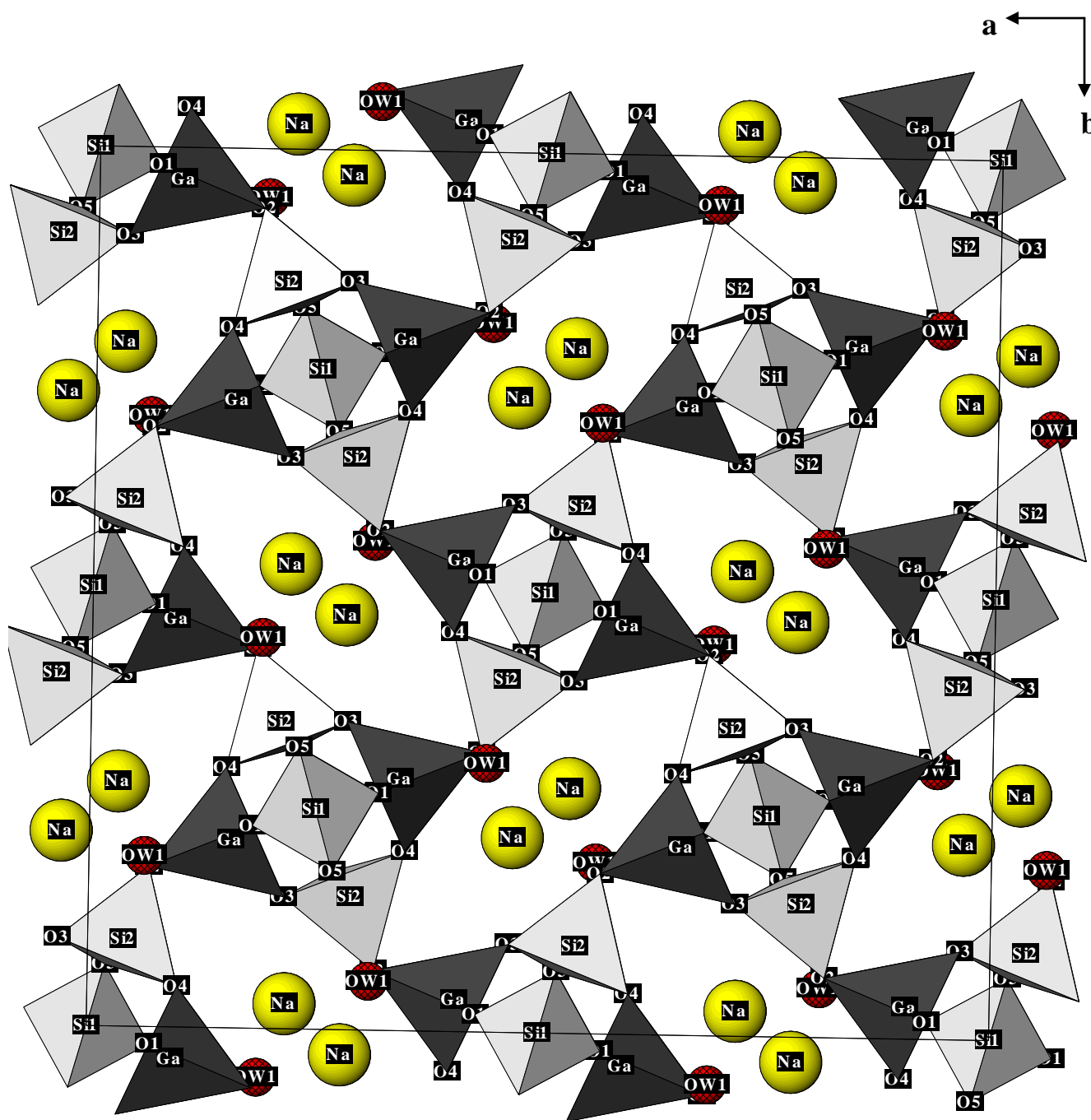


Figure 6: Graphical representation of orthorhombic gallosilicate natrolite at ambient temperature and pressure. Labelled atoms detail 3 T-sites: Si1; Si2 and Ga. Si tetrahedra (white), Ga tetrahedra (grey). Framework oxygens labelled as O1-5, water oxygen labelled as OW1.

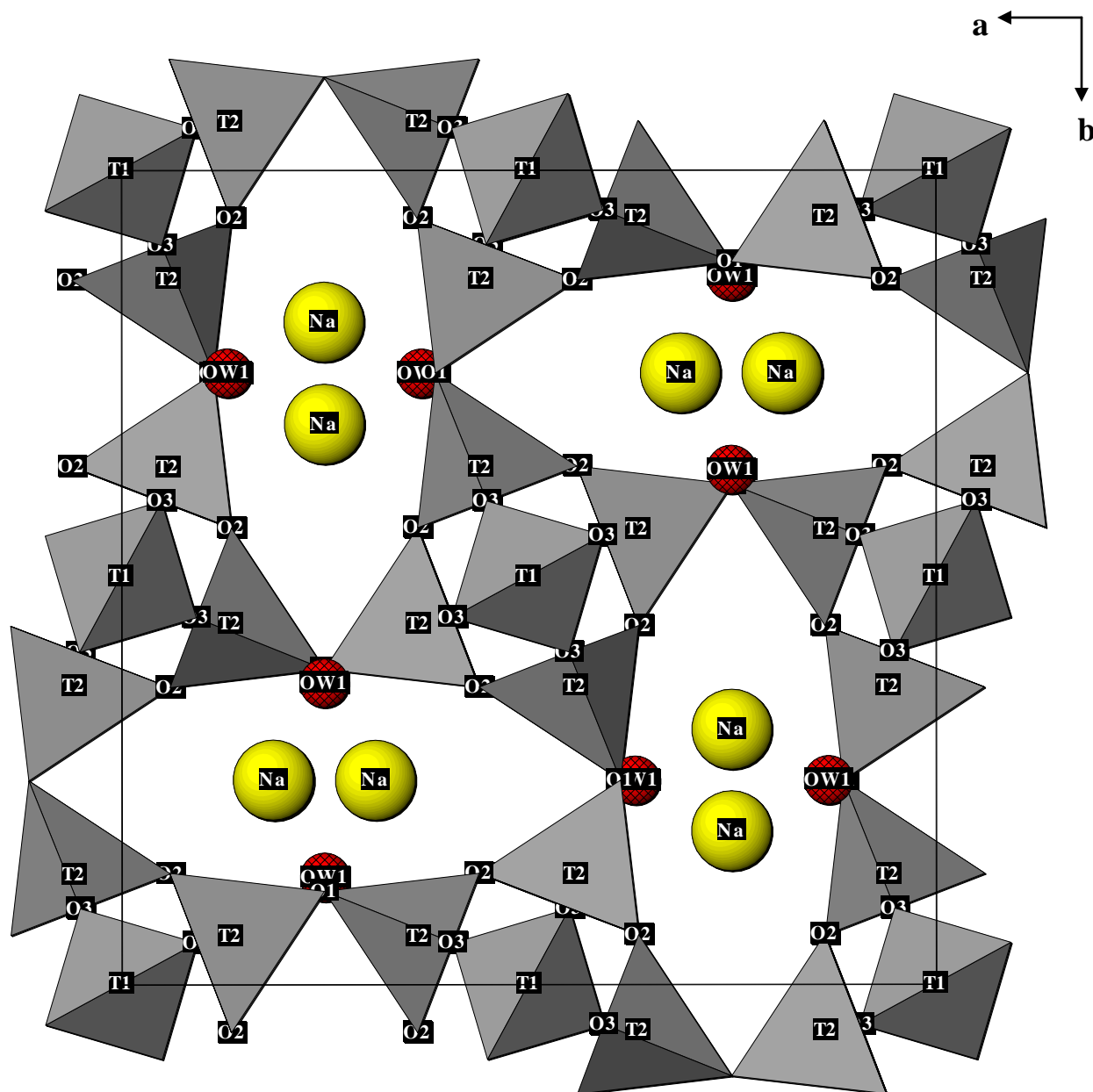


Figure 7: Graphical representation of tetragonal gallosilicate natrolite at ambient temperature and pressure. Labelled atoms detail 2 T-sites: T1 and T2. Disordered Si and Ga share each T-site in at 60% and 40% occupancy respectively. Framework oxygens labelled as O1-3, water oxygen labelled as OW1.

1.3 The Natrolite Family at High Pressure

The natrolite family is a group of zeolites which have shown evidence of pressure-induced phase transitions.^{7,11,17,18,19,20,21} These transitions are conditional upon pressure application and are completely reversible upon pressure release. Traditionally, temperature has been used to control the chemistry of zeolite pores, often resulting in the thermal decomposition of metastable structures at high temperatures or limiting mass transport effects at lower temperatures. When using pressure, both pore chemistry and crystal structure is influenced without any evidence of framework decomposition. For these reasons, the high-pressure behaviour of natrolite (and other related structures) is of significant interest. The nature of this high-pressure behaviour is described in the following sections.

1.3.1 Aluminosilicate Natrolite

The high pressure behaviour of aluminosilicate natrolite has been extensively investigated by Lee and co-workers.^{7,11,17,20,21} Upon high pressure application natrolite (Na- AlSi-NAT) shows an unexpected response. Pressures under $\sim 1\text{GPa}$ cause a predictable structure compression. However, at pressures in the region $0.8\text{--}1.25\text{GPa}$ there is a distinct, sharp increase in the volume of the unit cell ($\sim 2.5\text{--}7.0\%$).^{7,21} This response is coupled with an uptake of water into the pores. Figure 8 shows a summary of the high pressure phase transitions of natrolite. There are two distinct, reversible phase transitions under pressure. The first transition occurs at around 1.25GPa (as described above). This transition is to the paranatrolite form, a monoclinic cell with an extra 8 water molecules per unit and a volume increase of 7%. Increasing the pressure to 1.5GPa gives a second transition to the superhydrated form of natrolite. This involves a change of symmetry, back to the original orthorhombic cell. The transition to this phase is accompanied by the uptake of more water so that each unit has an extra 8 molecules (16 more than ambient

pressure natrolite). The unit cell of the superhydrated phase is approximately 2% larger than that of the original ambient pressure phase. At higher pressures natrolite tends towards a reversibly amorphous phase (between 7 and 10 GPa), with irreversible amorphisation occurring at pressures above 10 GPa.²²

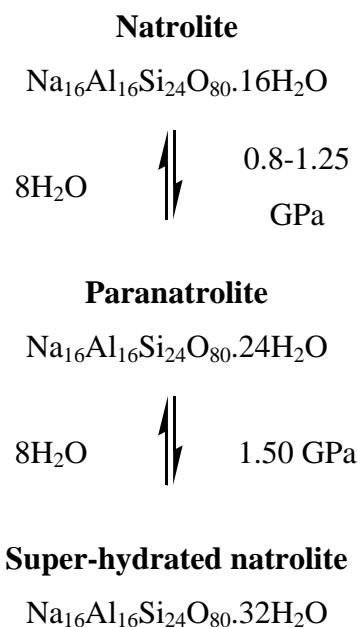


Figure 8: The reversible, pressure-induced phase transitions of natrolite.

Lee *et. al.*²¹ recorded powder X-ray diffraction data on natrolite as a function of pressure and analysed this to describe the structural changes accompanying this increase in cell volume and hydration. Addition of extra water molecules to the internal structure is facilitated by expansion of the zeolitic pores. Structurally, the expansion of natrolite under pressure can be described in terms of a rotation of the helical fibrous chains along the *c*-axis. Rotation of these chains causes a change in the angle of the bridging oxygen bond which connects the chains in the *a,b*-plane. The flexibility of this bond has been credited with facilitating pore opening/cell expansion. Rotation of the chains causes the elliptical pores of natrolite to become more open and circular in nature. It is this effect

which produces a net anisotropic volume increase by expansion along the *a*- and *b*-axis. This effect, termed ‘pressure-induced hydration’ (PIH), will be investigated throughout this thesis. Experiments upon the analogous zeotype, gallosilicate natrolite, will aim to investigate the occurrence and the nature of the PIH step. Comparison of the PIH step in the aluminosilicate and the gallosilicate natrolites will be used to determine the effects of Al/Ga framework substitution.

1.3.2 Tetranatrolite

Tetranatrolite, another member of the natrolite family, also exhibits pressure-induced hydration.¹⁸ Figure 9 shows a progression through the paranatrolite phase to the superhydrated phase, as seen in aluminosilicate natrolite. However, due to the compositional differences, the pressures of the transition points are very different to those observed in the Na-*AlSi*-NAT.

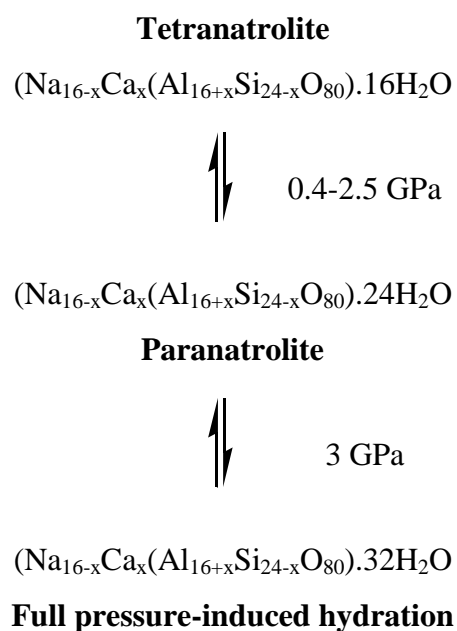


Figure 9: Pressure-induced hydration of tetranatrolite.¹⁸

1.3.3 Mesolite

Mesolite, also a member of the natrolite family, has the natrolite topology but with half the sodium cations substituted for calcium cations. Since calcium cations have a charge of 2^+ , as opposed to sodium which has a single positive charge; two charge balancing sodium cations can be replaced with just one calcium cation. This substitution frees up more space in the internal pore structure. This has a profound effect upon the high pressure behaviour. Figure 10 shows a summary of the high pressure behaviour of mesolite. Under pressure, mesolite undergoes a different transition to that described for natrolite. Instead of the paranatrolite and the superhydrated phases, a cation order/disorder is observed coupled with a preferential loss of Ca-coordinating water.²³ This transition occurs at 1.73 GPa and is accompanied by an expansion in the unit cell along the *a*- and *b*-axis. This expansion is much less in mesolite, 0.5%, when compared to natrolite.²¹ The transition seen in mesolite cannot be compared to that seen in natrolite, as dehydration rather than superhydration is observed.

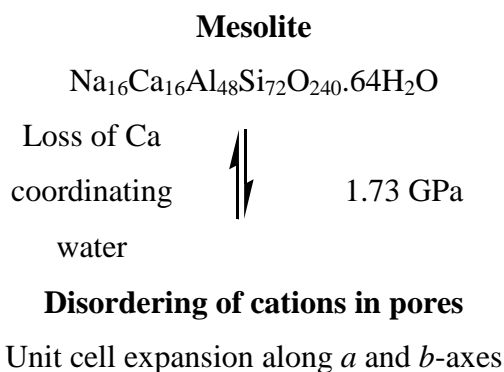


Figure 10: The reversible, pressure-induced phase transitions of mesolite.

1.3.4 Scolecite

Scolecite ($\text{Ca}_8\text{Al}_{16}\text{Si}_{24}\text{O}_{80}\cdot 24\text{H}_2\text{O}$), also a member of the natrolite family, has the natrolite topology but with all the sodium cations substituted by calcium cations. This substitution frees up yet more space in the internal pore structure when compared to mesolite.

Scolecite, like natrolite, is built from a series of fibrous chains extending in the *c*-axis direction. Scolecite differs from natrolite in the extra-framework cations, the water content and by rotation of the fibrous chains. In the 8-ring channels of scolecite there is only one cation site. This site is occupied by Ca which binds to three water molecules and four framework oxygens. Coordination to Ca forms a distorted pentagonal bipyramid. The fibrous chains of scolecite show a 22° rotation angle, relative to the *a,b*-axis; compared to natrolite and dehydrated natrolite at $23\text{-}24^\circ$ and 35° respectively.²⁴ Distortion of the fibrous chains acts to accommodate Ca^{2+} cations and an extra water molecule. This lowers the symmetry to monoclinic (*Cc* or *F1d1*) when compared to orthorhombic natrolite (*Fdd2*). These structural differences account for the difference in high pressure behaviour of scolecite; which shows no PIH at low pressures but does show pressure-induced amorphisation at high pressure (as seen in natrolite).

1.3.5 Gallosilicate Natrolite

Many of the members of the natrolite family have shown some form of interesting pressure-induced behaviour, so it was no surprise that a gallium silicate analogue of natrolite (K-GaSi-NAT), was reported by Lee *et. al.* as displaying PIH.^{20,21,25} The high pressure behaviour of K-GaSi-NAT is summarised in Figure 11.

In the case of K-GaSi-NAT the application of pressure shows an overall volume expansion, as well as an expansion of $\sim 0.4\%$ along the *c*-axis (whereas the analogous Na-AlSi-NAT shows a contraction along this axis). The most profound difference in the high pressure behaviour of K-GaSi-NAT is the irreversibility of the cell expansion. The expanded cell, which is assumed to be superhydrated, shows a $0.7\text{-}0.8\%$ increase in cell

volume. This expansion does not diminish upon pressure release, the first natrolite form to show an irreversible pressure-induced expansion. This behaviour is very interesting and would make an ideal specimen for further crystallographic research in this thesis. Unfortunately, contact with the authors revealed that synthesis of K-GaSi-NAT was un-reproducible. However, a recent report by Sun *et. al.* details the successful synthesis of K-GaSi-NAT.²⁶

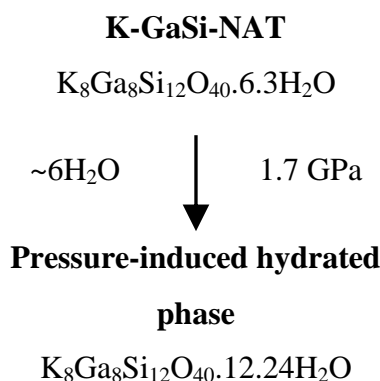


Figure 11: The irreversible pressure-induced phase transition of K-GaSi-NAT.²¹

Another gallosilicate natrolite (Na-GaSi-NAT), has also been reported as displaying pressure-induced hydration (Figure 12). Between 0.3 and 0.6 GPa Na-GaSi-NAT shows PIH with an expansion along the *a*- and *b*-axes as well as a contraction along the *c*-axis (as seen in Na-AlSi-NAT).¹⁹

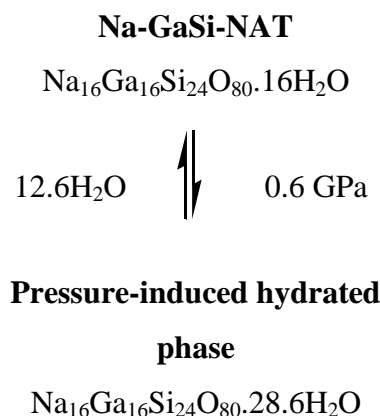


Figure 12: The reversible pressure-induced phase transition of Na-GaSi-NAT.¹⁹

Since this gallosilicate analogue displays similar behaviour to aluminosilicate natrolite, it would make an ideal candidate for zeolite↔zeoltype high pressure comparison. This preliminary study was the starting point for the work reported in this thesis. Two gallosilicate forms are included in these works: orthorhombic Na-GaSi-NAT and tetragonal Na-GaSi-NAT (differing only by the ordering of the T atom sites). To date there have not been *full* structural reports for these forms at ambient pressure and certainly none over a high pressure series.

1.4 Potential Uses of High-Pressure Superhydration: Aims of This Research

The more obvious potential uses of the pressure-induced hydration phenomenon are in controlled ion-exchange. A reversible increase in pore size, whilst under pressure, offers the potential for inserting a cation into the pore which would not normally ‘fit’ under ambient conditions. This application would be particularly useful when approaching the immobilisation of nuclear waste cations. Many organic and inorganic ion-exchange materials, both naturally occurring and synthetic, have been used and researched for the treatment of waste cations.^{27,28,29} Zeolites have been used in the British nuclear industry since 1985. British Nuclear Fuel Ltd. (BNFL), commissioned a dedicated site for the removal of nuclear waste via zeolite ion-exchange. The site, called SIXEP (site ion-exchange effluent plant), uses a naturally occurring zeolite, clinoptilolite. This zeolite is used to remove radionuclides (strontium and cesium ions) from fuel cooling pond water via ion-exchange. Clinoptilolite will readily exchange with cesium, strontium and many other ions, making it an ideal candidate for removal of ^{85}Sr and ^{134}Cs .^{30,31,32,33} This form of ion-exchange has been used for many years. The exchanged zeolite is not a permanent and complete form of immobilisation as exchanged cations can be leached from the solid. Often ‘spent’ immobilisation materials require encapsulation using a direct immobilisation matrix e.g. cement, bitumen and some polymers. The resultant matrix is

usually put into high integrity storage containers and buried at varying depths, depending upon the nature of the immobilised material. Generally zeolites offer a solidification matrix for the immobilisation of waste radionuclides and other toxic substances. Some recent reports have highlighted the use of natrolite in the removal of cyanide from waste water³⁴ and a mesolite analogue has been reported to remove uranium(VI), thorium(IV) and europium(III) from aqueous waste.³⁵

In the research reported in this thesis, it was hoped that the application of the PIH phenomenon to ion-exchange would provide an alternative radionuclide waste immobilisation method. The premise is that ion-exchange under high pressure conditions could produce a form of ‘cation-trapping’. Following ion-exchange of the superhydrated phase ion back-exchange/leaching would be suppressed upon pressure release. Both aluminosilicate and gallosilicate natrolites were studied. Full structural characterisation of the high pressure behaviour of the gallosilicate natrolites was completed before the ‘cation-trapping’ procedure was investigated.

1.4.1 Research Included in This Thesis:

- High pressure neutron diffraction of the gallosilicate natrolites

This method was used to characterise the systems at a limited number of high pressure steps. Neutron diffraction gives full structural details, including positions of hydrogen atoms from the intrapore water molecules. There is a publication by Colligan et al.¹⁷ which reports neutron diffraction structure characterisation of aluminosilicate natrolite, but none reporting the gallosilicate natrolites.

- High pressure synchrotron X-Ray diffraction

High pressure Synchrotron X-ray diffraction offers the opportunity to measure a large number of pressure steps at small pressure increments, and this was done for each gallosilicate material. This gives structural information complementary to the neutron diffraction data, but over a much greater range of pressures. These experiments clarify

the nature of the superhydration region and reveal a more exact pressure onset point. As mentioned earlier, there has been a preliminary report of high pressure synchrotron experiments performed upon orthorhombic gallosilicate natrolite,¹⁹ but it does not include the tetragonal gallosilicate form and does not report complimentary neutron diffraction experiments.

- High pressure ion-exchange

Aluminosilicate natrolite and both gallosilicate natrolite forms were used in bulk high-pressure ion-exchange experiments. Hydrothermal ion-exchange with a range of cations was used to select the best potential cation for use in ‘cation-trapping’ at high pressure. This high-pressure ‘cation-trapping’ method has never been reported (to date), and is demonstrated in this thesis, by the use of Quickpress equipment.

-
- ¹ Rabenau A. **1985**. *Angew. Chem. Int. Engl.* 24. 1026-1040
- ² Szostak R. 'Hand Book of Molecular Sieves' **1984**. *Van Nostrand Reinhold*. 6th Ed.
- ³ Gokel, G. W. 'Comprehensive supramolecular chemistry' **1996**. 7. 425-464.
- ⁴ Breck 'Zeolite Molecular Sieves' **1984**. *Krieger Publishing Company*.
- ⁵ Meier, W. M.; Olsen, D. H. 'Atlas of Zeolite Structures' **1987**. *Butterworths*. 2nd Ed.
- ⁶ IZA Structure Commission Database (www.iza-structure.org).
- ⁷ Lee Y.; Hriliac J. A.; Parise J. B.; Artioli G.; Vogt T. 'First structural investigation of a super-hydrated zeolite' **2001**. *J. Am. Chem. Soc.* 123. 12732-12733.
- ⁸ Artioli G.; Smith J. V.; Kvick Å. 'Neutron diffraction study of natrolite, Na₂Al₂Si₃O₁₀.2H₂O, at 20 K.' **1984** *Acta Cryst. C*40. 1658-1662.
- ⁹ Moroz N. K.; Kholopov E. V.; Belitsky I. A.; Furenko B. A. 'Pressure-enhanced molecular self-diffusion in microporous solids' **2001**. *Microporous and Mesoporous Materials*. 42. 113-119.
- ¹⁰ Evans Jr H. T.; Konnert J. A.; Ross M. 'The crystal structure of tetranatrolite from Mont Saint-Hilaire, Quebec, and its chemical and structural relationship to paranatrolite and gonnardite' **2000**. *American Mineralogist*. 85. 1808-1815.
- ¹¹ Lee Y.; Hriliac J. A.; Parise J. B.; Vogt T. 'Pressure-induced stabilisation of ordered paranatrolite: a possible solution to the paranatrolite controversy' **2005**. *American Mineralogist*. 90(1). 252-257.
- ¹² Ross M.; Marta M.; Flohr J.K.. 'Crystalline solution series and order-disorder within the natrolite mineral group' **1992**. *American Mineralogist*. 77. 685-703.
- ¹³ Pechar F. 'Structure refinement of Paranatrolite by X-ray diffraction' **1988**. *Cryst. Res. Technol.* 23(5). 647-653.
- ¹⁴ Hong S. B.; Kim S. H.; Kim Y. G.; Kim Y. C.; Barrett P. A.; Cambor M. A. 'Synthesis of microporous gallosilicates with the CGS topology' **1999**. *J. Mater. Chem.* 9. 2287.
- ¹⁵ Hong S. B.; Lee S. H.; Shin C.-H.; Woo A. J.; Alvarez L. J.; Zicovich-Wilson C. M.; Cambor M. A. 'In Situ Disorder-Order Transformation in Synthetic Gallosilicate Zeolites with the NAT Topology' **2004**. *J. Am. Chem. Soc.* 126(42). 13742-13751.

-
- ¹⁶ IZA Synthesis Commission ‘Adequate reporting of zeolite synthesis in the literature’ **1993**. *13*. 399-402.
- ¹⁷ Colligan M.; Lee Y.; Vogt T.; Celestian A. J.; Paris J. B.; Marshall W. B.; Hriljac J. A. ‘High-pressure neutron diffraction study of superhydrated natrolite.’ **2005**. *J. Phys. Chem. B*. *109*. 18223-18225.
- ¹⁸ Lee Y.; Hriljac J. A.; Parise J. B.; Vogt T. ‘Pressure-induced hydration in zeolite tetranatrolite’ **2006**. *J. Am. Chem. Soc.* *91*. 247-251.
- ¹⁹ Lee Y.; Hriljac J. A.; Kim S. J.; Vogt T.; Hanson, J. C. ‘Pressure-induced hydration at 0.6 GPa in a synthetic gallosilicate zeolite’ **2003**. *J. Am. Chem. Soc.* *125*. 6036-6037.
- ²⁰ Lee Y.; Vogt T.; Hriljac J. A.; Parise J. B.; Hanson J. C.; Kim S. ‘Non-framework cation migration and irreversible pressure-induced hydration in a zeolite’ **2002**. *Letters to Nature*. *420*. 485-489.
- ²¹ Lee Y.; Hriljac J. A.; Kim S. J.; Vogt T.; Parise J. B.; Artioli G. ‘Pressure-induced volume expansion of zeolites in the Natrolite family’ **2002**. *J. Am. Chem. Soc.* *124*. 5466-5475.
- ²² Groyainov S. ‘Pressure-induced amorphisation of $\text{Na}_2\text{Al}_2\text{Si}_3\text{O}_{10}\cdot 2\text{H}_2\text{O}$ and KAlSi_2O_6 ’ **2005**. *Physica Status Solidi*. *202*. N°3. 25-27.
- ²³ Stahl K.; Hanson J. **1994**. *J. Appl. Crystallogr.* *27*. 543-550.
- ²⁴ Comodi P.; Gatta G. D.; Zanazzi P. F. ‘High-pressure structural behaviour of scolecite’ **2002**. *Eur. J. Mineral* *14*. 567-574.
- ²⁵ Lee Y.; Kim S. J.; Parise J. B. ‘Synthesis and crystal structures of gallium- and germanium- variants of the fibrous zeolites with the NAT, EDI and THO structure types’ **2000**. *Microporous and Mesoporous Materials*. *34*. 255-271.
- ²⁶ Sun P.; Navrotsky A. ‘Formation and dehydration enthalpy of gallosilicate zeolites’ **2008**. *Microporous and Mesoporous Materials*. *111*. 507–516.
- ²⁷ International Atomic Energy Agency, Vienna **2002**. *Technical Reports series* N°408.
- ²⁸ Koivula R. ‘Inorganic ion exchangers for decontamination of radioactive wastes generated by the nuclear power plants’ **2004** *Report Series in Radiochemistry*. *23*. Helsinki.

-
- ²⁹ Moller T. 'Selective Crystalline Inorganic Materials as Ion Exchangers in the Treatment of Nuclear Waste Solutions' Academic Dissertation. **2002**. *University of Helsinki, Finland*.
- ³⁰ Rodriguez-Iznaga, I.; Gomez A.; Rodriguez-Fuentes G.; Benitez-Anguilar A.; Serrano-Ballan J. 'Natural clinoptilolite as an exchanger of Ni^{2+} and NH_4^+ ions under hydrothermal conditions and high ammonia concentration' **2002** *Microporous and Mesoporous Materials*. 53. 71-80.
- ³¹ Woods R. M.; Gunter M. E. 'Na- and Cs- exchange in a clinoptilolite-rich rock: Analysis of the outgoing cations in solution' **2001**. *American Mineralogist*. 86. 424-430.
- ³² Palmer J. L.; Gunter M. E. 'The effects of time, temperature, and concentration on Sr^{2+} exchange in clinoptilolite in aqueous solutions' **2001**. *American Mineralogist*. 86. 431-437.
- ³³ Kazemian H.; Modarres H.; Ghasemi Mobtaker H. 'Iranian natural clinoptilolite and its synthetic zeolite P for removal of cerium and thorium from nuclear wastewaters' **2003** *Journal of Radioanalytical and Nuclear Chemistry*. 258 (3). 551-556.
- ³⁴ Noroozifar M.; Khorasani-Motlagh M.; Ahmadzadeh Fard P. 'Cyanide uptake from wastewater by modified natrolite zeolite-iron oxyhydroxide system: Application of isotherm and kinetic models' **2009**. *Journal of Hazardous Materials*. 166. 1060-1066.
- ³⁵ Sharma P.; Tomar R. 'Synthesis and application of an analogue of mesolite for the removal of uranium(VI), thorium(IV), and europium(III) from aqueous waste' **2008**. *Microporous and Mesoporous Materials*. 116. 641-652.